



# Nodal schemes, mixed-hybrid finite elements and block-centered finite differences

Jean-Pierre Hennart

## ► To cite this version:

Jean-Pierre Hennart. Nodal schemes, mixed-hybrid finite elements and block-centered finite differences. RR-0386, INRIA. 1985. inria-00076170

**HAL Id: inria-00076170**

**<https://inria.hal.science/inria-00076170>**

Submitted on 24 May 2006

**HAL** is a multi-disciplinary open access archive for the deposit and dissemination of scientific research documents, whether they are published or not. The documents may come from teaching and research institutions in France or abroad, or from public or private research centers.

L'archive ouverte pluridisciplinaire **HAL**, est destinée au dépôt et à la diffusion de documents scientifiques de niveau recherche, publiés ou non, émanant des établissements d'enseignement et de recherche français ou étrangers, des laboratoires publics ou privés.



CENTRE DE ROCQUENCOURT

Institut National  
de Recherche  
en Informatique  
et en Automatique

Domaine de Voluceau  
Rocquencourt  
B.P. 105

78153 Le Chesnay Cedex  
France

Tél. (3) 954 90 20

Rapports de Recherche

N° 386

**NODAL SCHEMES,  
MIXED-HYBRID  
FINITE ELEMENTS  
AND BLOCK-CENTERED  
FINITE DIFFERENCES**

**Jean-Pierre HENNART**

**Mars 1985**

NODAL SCHEMES,  
MIXED-HYBRID FINITE ELEMENTS  
AND BLOCK-CENTERED FINITE DIFFERENCES

-*Jean-Pierre* HENNART -

IIMAS-UNAM

*Apartado Postal 20-726*  
01000 México, D.F. (MEXICO)

Professeur invité dans le projet de M. CHAVENT du 1.4.84 au 31.7.84.

## RESUME

Les relations existant entre une famille générale de schémas nodaux introduite récemment (J.P. Hennart, SIAM J. on Scientific and Statistical Computing, à paraître) et les formulations en éléments finis mixtes hybrides étudiées par D.N. Arnold et F. Brezzi (RAIRO - Numerical Analysis, à paraître) sont explorées dans cet article : on montre en particulier que les schémas nodaux proposés sont les extensions les plus naturelles en géométrie rectangulaire des éléments finis mixtes-hybrides de Raviart-Thomas-Nédélec, et qu'ils sont de plus en relation directe avec les schémas aux différences finis de type bloc-centrés, fournissant ainsi incidemment une classe utile de préconditionneurs.

## ABSTRACT

The relationship between a general family of nodal schemes introduced recently (J.P. Hennart, SIAM J. on Scientific and Statistical Computing. To Appear) and mixed-hybrid finite element formulations as studied by D.N. Arnold and F. Brezzi (RAIRO - Numerical Analysis. To Appear) are explored in this paper : it is shown in particular that the nodal schemes proposed are the most natural extensions in rectangular geometry of the Raviart-Thomas-Nédélec mixed-hybrid finite elements, and that they are moreover directly related to block-centered finite differences schemes, providing incidentally a potentially usefull class of preconditioners.

## MOTS-CLES

Eléments finis - Différences finies - Méthodes nodales .

## KEY WORDS

Finite elements - Finite differences - Nodal methods.

## 1. INTRODUCTION

---

Modern coarse-mesh or nodal methods were developed in the 1970's in numerical nuclear reactor calculation. (See for instance the recent review paper by J. Dorning<sup>1</sup>). Roughly speaking, nodal methods are fast and accurate methods which try to combine the attractive features of the finite difference method (f.d.m.) and of the finite element method (f.e.m.). From the f.e.m., they borrow a piecewise continuous, usually polynomial, behavior over a given coarse mesh. With the f.d.m., they have in common the fact that the final algebraic systems are usually quite sparse and well structured, at least over domains not too irregular like unions of rectangles: in the same situation, classical conforming finite elements would typically lead to much more coupled systems of equations. Nodal methods can thus be viewed as fast solvers, amenable to recent techniques of vectorization and (or) parallelism. They are specially suited to all physical situations which have been traditionally modelled by finite differences, and for which the domain as well as the coefficients of the equation are not known with sufficient accuracy: it is then tempting to use a regular rectangular grid to discretize the domain and to assume that over each "block", "cell", "node" or "element" of the grid the physical parameters are not known with great accuracy, so that a constant or mean value only is available. This situation is prevailing for instance in groundwater hydrology, oil reservoir simulation, air pollution modelling problems, etc.

In the reservoir simulation field for instance, where the industrial simulators are almost exclusively based on the f.d.m. over rectangular grids, it would be quite attractive to develop fast, accurate and mathematically well-founded nodal schemes over such grids, especially for three-dimensional situations. Recently<sup>2</sup>, we analyzed some early nodal schemes and related them to nonstandard nonconforming finite element schemes. We also explained why these simplest original schemes are not quite satisfactory, in the sense that they do not climb correctly in degree. This was corrected later<sup>3</sup> when a new and more general family of nodal schemes was introduced, which do not exhibit that defect. General considerations typical of the analysis of nonconforming schemes led us<sup>3</sup> to the conclusion that the nodal scheme of type (k) for some index  $k \in \mathbb{N}$  should exhibit errors in norm  $L_2$  of  $O(h^{k+2})$ , as numerical experiments did confirm<sup>4</sup>. The corresponding error estimates will be proved here rigorously in a somewhat indirect way.

Most of the experimental computer codes which tried during the last few years to convince the petroleum engineers of the merits of finite elements in reservoir simulation<sup>5,6</sup> are based on the mixed finite element formulation. In such a formulation, the unknown function (here the pressure  $p$ ) and its current (the corresponding Darcy velocity  $\tilde{v}$ ) are computed simultaneously without differentiation of  $p$  and multiplication by a rough

coefficient. This is particularly suitable, since only the velocity and not the pressure appears in the concentration (resp. saturation) equations, if the displacement considered is miscible (resp. immiscible). Moreover the velocity field varies more slowly in time and space than either the pressure or the concentration (resp. saturation) fields, and is therefore the correct variable to pick up. The trouble with the mixed formulation is that it generally leads to indefinite algebraic systems. As discussed in a recent paper by Arnold and Brezzi <sup>7</sup>, a standard way to remove this difficulty consists of using a mixed-hybrid formulation, whereby the interelement continuity is imposed through the use of Lagrange multipliers. The resulting systems are positive definite. Arnold and Brezzi show moreover that the computed multipliers can be used in an elementwise postprocessing operation, which enhances the accuracy of the original approximation.

In Section 2, we shall introduce some notations and recall the general family of nodal schemes we introduced earlier <sup>3</sup>, presenting it as a nonconforming f.e.m.. In Section 3, the mixed and mixed-hybrid formulations are introduced. For rectangular meshes, a set of basis functions is given, which turns out to be particularly convenient when later it is proved that the nodal schemes introduced in Section 2 can be

obtained through the postprocessing operation mentioned earlier, if the Raviart-Thomas-Nédélec spaces <sup>8,9</sup> are used in the mixed-hybrid formulation. As in Arnold and Brezzi <sup>7</sup>, this fact is exploited to provide error estimates in Section 4. In Section 5, this mixed-hybrid formulation with postprocessing is compared with the original nonconforming one in the rectangular case and some details of implementation are discussed. Finally, Section 6 explores the relationship between the nodal schemes of Section 2 and block-centered finite difference schemes.

It is fair to say that most of the technical details are adapted from the excellent paper by Arnold and Brezzi <sup>7</sup>, which was restricted to the triangular case. In this paper, the emphasis is on the rectangular case, where it turns out that the extensions proposed by Arnold and Brezzi <sup>7</sup> of the mixed-hybrid approximations within the Raviart-Thomas-Nédélec spaces are directly related to the nodal schemes we introduced <sup>3</sup>. Realizing it leads us easily to error estimates and also to an implementation which is intrinsically easier and more robust than the original one.

In the following sections, we shall restrict ourselves to the typical second order elliptic equation



$$Lu := -\operatorname{div}(\underline{a} \operatorname{grad} u) + bu = f \quad \text{on} \quad \Omega \subset \mathbb{R}^2, \quad (1.1a)$$

subject to homogeneous Dirichlet boundary conditions

$$u = 0 \quad \text{on} \quad \Gamma, \quad (1.1b)$$

where  $\Gamma = \overline{\Omega} - \Omega$ . In (1.1a), the diffusion tensor  $\underline{a}$  is a two by two matrix-valued function on  $\Omega$  assumed to be positive definite, i.e. there exists  $\alpha > 0$  such that

$$\sum_{i,j=1}^2 \underline{a}_{ij}(x) \xi_i \xi_j \geq \alpha \|\xi\|^2, \quad \forall x \in \Omega \text{ \& \; } \forall \xi \in \mathbb{R}^2. \quad (1.2)$$

We shall denote by  $\underline{c}$  the inverse of the diffusion tensor:

$$\underline{c} := \underline{a}^{-1}. \quad (1.3)$$

Finally  $f$  and  $b$  are given functions in  $L^2(\Omega)$ ,  $b$  being moreover nonnegative. In the following, we shall always assume that the coefficients of the equations and  $\underline{a}$  in particular are sufficiently smooth to ensure that  $u$  has enough regularity, depending on the particular context considered. A last function we shall often use is the flux  $\underline{p}$  associated to  $u$ , namely

$$\underline{p} := - \underline{a} \operatorname{grad} u. \quad (1.4)$$

The classical primal variational formulation of problem (1.1) consists in finding  $u \in V = H_0^1(\Omega)$  such that

$$a(u, v) = f(v) \quad , \quad \forall v \in V \quad , \quad (1.5a)$$

where  $a(\cdot, \cdot)$  and  $f(\cdot)$  are the following bilinear and linear forms

$$a(u, v) = \int_{\Omega} \left( \sum_{i,j=1}^2 a_{ji} \partial_i u \partial_j v + buv \right) dx \quad , \quad (1.5b)$$

and

$$f(v) = \int_{\Omega} f v dx \quad . \quad (1.5c)$$

A conforming approximation of  $u$  is obtained by looking for  $u_h \in V_h \subset H_0^1(\Omega)$  with  $\dim V_h < \infty$  such that

$$a(u_h, v_h) = f(v_h) \quad , \quad \forall v_h \in V_h \quad . \quad (1.6)$$

## 2. NODAL SCHEMES AS NONCONFORMING FINITE ELEMENTS

For the sake of simplicity, we shall consider a domain  $\Omega \subset \mathbb{R}^2$  which is of the type "union of rectangles", in other words it can be discretized exactly by a rectangular grid  $R_h$  with cells  $C$  whose boundary  $\partial C$  consists of four edges denoted espezifically by  $L$ ,  $R$ ,  $B$  and  $T$  (for Left, Right, Bottom and Top), or by  $E$  generically. Each particular cell will be referred by a unique invertible affine mapping to the reference cell  $\hat{C} \equiv [-1, +1] \times [-1, +1]$ , which we will not distinguish from  $C$  when no confusion is possible.

The general family of nodal schemes introduced earlier<sup>3</sup> is in fact a family of nonconforming elements in  $H^1(\Omega)$  defined by:

$K$  a domain which will always be in our case a rectangular cell  $C$  or rather its affine equivalent square cell  $\hat{C}$ ;

$S$  a space of polynomials  $p$  on  $K$  of dimension  $N$ ;

$D$  a set of  $N$  degrees of freedom which are linear functionals  $\ell$  acting on  $S$ .

A finite element of this family is said to be unisolvent if

$$\ell(p) = 0 \quad , \quad \forall \ell \in D \quad \text{and} \quad p \in S \Rightarrow p \equiv 0 \quad . \quad (2.1)$$

Let us introduce the following elementary spaces of polynomials:

$$Q^{k,1}(K) \equiv \{x^i y^j, 0 \leq i \leq k, 0 \leq j \leq 1\} \quad \text{on } K, \quad (2.2a)$$

$$Q^k(K) \equiv Q^{k,k}(K), \quad (2.2b)$$

and

$$P^k(K) \equiv \{x^i y^j, 0 \leq i+j \leq k\} \quad \text{on } K, \quad (2.2c)$$

as well as the linear forms associated to the cell  $C$

$$m_C^{ij}(u) = \int_C P_i(x) P_j(y) u(x,y) dx dy / N_i \cdot N_j, \quad (2.3a)$$

$$i, j \in \mathbb{N}, \quad \forall u \in L^2(C),$$

and to its faces  $L, R, B$  and  $T$

$$m_L^i(u) = \int_L P_i(y) u(-1, y) dy / N_i,$$

$$m_R^i(u) = \int_R P_i(y) u(+1, y) dy / N_i,$$

$$m_B^i(u) = \int_B P_i(x) u(x, -1) dx / N_i,$$

and  $m_T^i(u) = \int_T P_i(x) u(x, +1) dx / N_i,$

where  $N_i = 2/(2i+1) = \int_{-1}^{+1} P_i^2 dx$  is a convenient normalization

factor while  $P_i$  is the normalized Legendre polynomial over  $[-1, +1]$

For a nodal scheme of type  $(k)$ ,  $k \in \mathbb{N}$

$$S = N^k(K) := Q^{k+2,k} \cup Q^{k,k+2} \quad \text{on } K$$

$$\dim N^k = (k+1)(k+5) \quad , \quad (2.4a)$$

$$D = \mathcal{DN}^k(K) := \{m_L^i(u_h), m_R^i(u_h), m_B^i(u_h), m_T^i(u_h) \quad , \quad i=0, \dots, k ;$$

$$m_C^{ij}(u_h) \quad , \quad i, j=0, \dots, k\} \quad \text{on } K \quad ,$$

$$\text{card } \mathcal{DN}^k = (k+1)(k+5) \quad . \quad (2.4b)$$

It has been shown <sup>3</sup> that the finite elements of this family are unisolvent for any  $k$ : this was done by exhibiting the corresponding basis functions. Thanks to the choice of  $\hat{C}$  as a reference element and to the use of normalized Legendre polynomials, these basis functions can be expressed in an especially simple and compact form, which was given<sup>3</sup> in one, two and three dimensions, as well as in the case where different degrees of approximation are considered in the different directions. We refer the interested readers to Ref. 3, Section 3 and Appendices A, B and C for more details. Here, for the sake of simplicity, we shall only recall the basis functions for the 2D case. Corresponding to the degrees of freedom  $m_L^i$ ,  $m_R^i$ ,  $m_B^i$ ,  $m_T^i$  and  $m_C^{ij}$  of  $u_h$ , we have the following basis functions

$$u_L^i(x,y) = \frac{1}{2} (-1)^{k+1} \left[ P_{k+1}(x) - P_{k+2}(x) \right] P_i(y) , \quad i=0,\dots,k , \quad (2.5a)$$

$$u_R^i(x,y) = \frac{1}{2} \left[ P_{k+1}(x) + P_{k+2}(x) \right] P_i(y) , \quad i=0,\dots,k , \quad (2.5b)$$

$$u_B^i(x,y) = \frac{1}{2} (-1)^{k+1} P_i(x) \left[ P_{k+1}(y) - P_{k+2}(y) \right] , \quad i=0,\dots,k , \quad (2.5c)$$

$$u_T^i(x,y) = \frac{1}{2} P_i(x) \left[ P_{k+1}(y) + P_{k+2}(y) \right] , \quad i=0,\dots,k , \quad (2.5d)$$

and

$$u_C^{ij}(x,y) = P_i(x)P_j(y) - P_{k+1(i)}(x)P_j(y) - P_i(x)P_{k+1(j)}(y) , \quad i,j=0,\dots,k , \quad (2.5e)$$

where  $1(i)$  (resp.  $1(j)$ ) = 1 or 2 and is such that  $i$  and  $k+1(i)$  (resp.  $j$  and  $k+1(j)$ ) have the same parity.

Let us define

$$N_{-1}^k(R_h) = \left\{ u_h \mid u_h \in L^2(\Omega) , \quad u_h|_K \in N^k(K) , \quad \forall K \in R_h , \right.$$

the moments  $m_L^i, \dots, m_T^i$ ,  $i=0, \dots, k$  are

continuous across the interfaces

between different cells and are 0

on boundary edges  $\left. \vphantom{\begin{matrix} \text{the moments} \\ \text{continuous across the interfaces} \\ \text{between different cells and are 0} \end{matrix}} \right\} . \quad (2.6)$

The elements of this space are nodal functions of type  $(k)$ , which are clearly nonconforming in  $H^1(\Omega)$ , since only their moments are continuous at interelement boundaries but not the function itself (whence the subscript  $-1$ ). On the other hand, the moment continuity conditions ensure that the "patch test"<sup>10,11</sup> is passed at its lowest order for any  $k$  and that a super patch test is passed if  $k > 0$ .

Let us mention finally that

$$P^{k+2-\delta_{k0}} \subset N^k, \quad \forall k \in \mathbb{N}, \quad (2.7)$$

where  $\delta_{k0}$  is the usual Kronecker symbol.

Since  $V_h := N_{-1}^k(R_h) \not\subset H_0^1(\Omega)$ , a nonconforming approximation  $u_h$  of  $u$  based on the primal variational formulation (1.5) is now obtained by slightly modifying (1.6), namely we look for  $u_h \in V_h \not\subset H_0^1(\Omega)$  such that

$$a_h(u_h, v_h) = f(v_h), \quad \forall v_h \in V_h, \quad (2.8a)$$

where

$$a_h(u, v) = \sum_C \int_C \left( \sum_{i,j=1}^2 a_{ji} \partial_i u \partial_j v + buv \right) dx. \quad (2.8b)$$

In the following this approximation of  $u$  will be referred to as the mathematical nodal method (m.n.m.) of index  $k$ .

To each m.n.m. corresponds a p.n.m. (for physical nodal method) which is obtained from the same  $V_h$  as above, but where the final algebraic equations are derived from *physical* considerations; namely, one expresses that weighted balance equations are satisfied over the cell for all weights  $w(x,y) \in Q^k(K)$  ( $(k+1)^2$  equations) and that the mean values and moments up to order  $k$  of the normal fluxes  $p_{\tilde{h}}$  are continuous through the faces of the nodes ( $4(k+1)$  equations), the mean values and moments of  $u_h$  being already continuous by construction. In Ref. 3, we proved that the p.n.m. of index  $k$  was in fact a m.n.m. of the same index where the matrix elements are calculated in an approximate way by using a numerical quadrature of the Radau type *in a nonstandard way*. In view of the importance in the next sections of these arguments, we shall repeat them here. First of all, we should clarify what we mean by *nonstandard* Radau quadrature: for a given index  $k \in \mathbb{N}$ , the Radau quadrature points  $x_R$  are the  $(k+2)$  zeros of  $P_{k+2}(x) \pm P_{k+1}(x)$  including  $x = \pm 1$ . In 2D, a product Radau quadrature would be exact for polynomials belonging to  $Q^1$  where  $1 = 2k+2$ , and would in particular integrate exactly the stiffness matrix, provided  $a$  is piecewise constant. For mass matrices, each time an edge basis function appears like  $u_E$ ,



where  $E=L,R,B$  or  $T$ , the opposite Radau quadrature points should be used, namely  $x_R^R, x_R^L, y_R^T$  and  $y_R^B$ , so that the elementary mass matrix only has nonzero entries for the cell moment elements like  $(u_C^{ij}, u_C^{kl})$ . For these matrix elements, the asymmetry inherent to the Radau rules is restored by using the relationship

$$\begin{aligned} P_1(x)P_m(y) \equiv P_{1m}(x,y) = & (-1)^1 u_L^m(x,y) + u_R^m(x,y) \\ & + (-1)^m u_B^1(x,y) + u_T^1(x,y) \\ & + u_C^{1m}(x,y) \quad , \quad l,m=0,\dots,k \quad , \quad (2.9) \end{aligned}$$

so that with Radau quadrature points

$$(u_C^{ij}, u_C^{kl}) = (P_{ij}, P_{kl}) = \frac{4}{(2i+1)(2j+1)} \delta_{ik} \delta_{jl} \quad , \quad (2.10)$$

since the Radau rule is correct for  $x^\alpha y^\beta$ ,  $\alpha, \beta \leq 2k+2$ . In the case  $k=0$  for instance, the Radau quadrature leads to

$$(u_C^{00}, u_C^{00}) = 4.0 \quad , \quad (2.11)$$

and not to 5.6 as analytical integration would do. An interpretation of this in terms of some  $L^2$ - projection will be given bellow.

The following general theorems can be proved:

THEOREM 1 The p.n.m. of index  $k$  is equivalent to the m.n.m. of the same index if *nonstandard Radau integration* is used.

Proof:

The m.n.m. consists of finding  $u_h \in V_h$  such that

$$a_h(u_h, v_h) = f(v_h) \quad , \quad \forall v_h \in V_h \quad , \quad (2.12)$$

where

$$a_h(u_h, v_h) = \sum_C \int_C \left( \sum_{i,j=1}^2 a_{ji} \partial_i u_h \partial_j v_h + b u_h v_h \right) dx \quad , \quad (2.13)$$

and

$$f(v_h) = \int_{\Omega} f v_h \, dx \quad . \quad (2.14)$$

a. Let us take as  $v_h$  the cell basis functions  $u_C^{mn}$ ,  $m, n=0, \dots, k$ , associated to some cell  $C$ . Eq. (2.12) becomes

$$\int_C \left( \sum_{i,j=1}^2 a_{ji} \partial_i u_h \partial_j u_C^{mn} + b u_h u_C^{mn} - f u_C^{mn} \right) dx = 0 \quad , \quad (2.15)$$

$m, n=0, \dots, k \quad ,$

or equivalently

$$\int_{\partial C} u_C^{mn} \sum_{i,j=1}^2 a_{ji} \partial_{ih} u_{hj} \cdot ds$$

$$+ \int_C u_C^{mn} (-\operatorname{div}(\underline{a} \operatorname{grad} u_h) + b u_h - f) dx = 0, \quad m, n = 0, \dots, k. \quad (2.16)$$

Let us first show that the boundary term  $\int_{\partial C} \underline{\quad}$  is zero:  
 with (2.9), it is easy to rewrite  $u_h \in V_h$  as

$$u_h = \sum_{p=0}^k \sum_{q=0}^k m_C^{pq} P_{pq}(x, y)$$

$$+ \sum_{p=0}^k \left[ m_L^{p*} u_L^p(x, y) + m_R^{p*} u_R^p(x, y) + m_B^{p*} u_B^p(x, y) + m_T^{p*} u_T^p(x, y) \right], \quad (2.17)$$

so that the contribution of the  $P_{pq}$  terms to the normal gradient on the boundary will be proportional at most to  $P_q(y)$  and  $P_p(x)$ ,  $p, q \leq k$ .

From (2.5e), it is easily seen that on  $\partial C$ ,  $u_C^{mn}$  reduces to

$$u_C^{mn}(x, \pm 1) \propto P_{k+1(m)}(x),$$

and

(2.19)

$$u_C^{mn}(\pm 1, y) \propto P_{k+1(n)}(y),$$

where  $l(m)$  and  $l(n)=1$  or  $2$ . If we assume that  $a_{ji}$  is constant over a given cell, the corresponding boundary terms are zero as  $u_C^{mn}$  is orthogonal on the boundary to  $P_q(y)$  and  $P_p(x)$ ,  $p, q \leq k$ . The Radau quadrature rule would integrate exactly these products and give the correct zero answer. Notice that the same result would be obtained *independently of the  $a_{ji}$ 's* if we were to use on the boundary a Gauss quadrature rule with  $k+1(m)$  or  $k+1(n)$  Gauss points.

The contributions of the edge basis functions to the normal gradient on the boundary are easily seen to be proportional to  $P_p(x \text{ or } y)$ ,  $p \leq k$  or to  $P_{k+1} \pm P_{k+2}(x \text{ or } y)$ . In the first case, the corresponding boundary terms are zero for the same reason as above while in the second case they disappear thanks to the Radau quadrature rule. Eq. (2.16) finally becomes under Radau quadrature,

$$\int_C P_{lm} (-\text{div}(\underline{a} \text{ grad } u_n) + b u_h - f) dx = 0, \quad l, m = 0, \dots, k, \quad (2.20)$$

which is the equivalent to the cell balance equation with respect to all weights  $w(x, y) \in Q^k(K)$ .

b. Let us now take as  $v_h$  the edge basis functions  $u_E^m$ ,  $m=0, \dots, k$  where  $E=L, R, B$  or  $T$ . For the sake of simplicity, let us consider  $u_E^m$  reducing to  $u_R^m$  on  $K_1$  and to  $u_L^m$  on  $K_2$  with  $\Gamma_{12} = \overline{K}_1 \cap \overline{K}_2$ . For this particular example, Eq. (2.12) becomes

$$\begin{aligned} & \int_{K_1} \left( \sum_{i,j=1}^2 a_{ji} \partial_i u_h \partial_j u_R^m + b u_h u_R^m - f u_R^m \right) dx \\ & + \int_{K_2} \left( \sum_{i,j=1}^2 a_{ji} \partial_i u_h \partial_j u_L^m + b u_h u_L^m - f u_L^m \right) dx = 0, \\ & m=0, \dots, k, \end{aligned} \quad (2.21)$$

or equivalently after Radau quadrature

$$\begin{aligned} & \int_{\partial K_1} u_R^m \sum_{i,j=1}^2 a_{ji} \partial_i u_h l_j \cdot ds + \int_{\partial K_2} u_L^m \sum_{i,j=1}^2 a_{ji} \partial_i u_h l_j \cdot ds = 0, \\ & m=0, \dots, k. \end{aligned} \quad (2.22)$$

Since  $u^m$  is either zero ( $u_R^m$  on  $L_1$  and  $u_L^m$  on  $R_2$ ) or because of Radau quadrature on  $B_1$ ,  $T_1$ ,  $B_2$  and  $T_2$ , (2.22) reduces to

$$\begin{aligned} & \int_{\Gamma_{12}} p_m(y) \left[ \sum_{i=1}^2 a_{ji} \partial_i u_h \Big|_{K_1} - \sum_{i=1}^2 a_{ji} \partial_i u_h \Big|_{K_2} \right] l_x \cdot dy = 0, \\ & m=0, \dots, k, \end{aligned} \quad (2.23)$$

and is therefore equivalent to the continuity conditions of the mean values and moments up to order  $k$  of the normal fluxes  $p_h$ . ■

Let us introduce

$$U_{-1}^k(R_h) = \{u_h \mid u_h \in L^2(\Omega), u_h|_K \in Q^k(K), \forall K \in R_h\}, \quad (2.24)$$

which turns out to be the space where  $u$  shall be looked for in the next section when mixed finite elements will be introduced. We have

**THEOREM 2** The nonstandard Radau integration introduced hereabove is equivalent to an  $L^2$  projection from  $N_{-1}^k(R_h)$  onto  $U_{-1}^k(R_h)$ .

Proof:

Evident when one realizes that the use of the Radau points filters out all the components outside  $Q^k(K)$ , like the edge basis functions  $\propto P_{k+1} \pm P_{k+2}$ . The way the quadrature is used for the cell basis functions with (2.9) shows moreover that only the  $P_{lm}$  component  $\in Q^k(K)$  are kept. ■

### 3. MIXED AND MIXED-HYBRID FORMULATIONS

The basis of mixed formulations for problem (1.1) consists in rewriting (1.1a) as a coupled set of lower order equations, namely

$$\underline{c} \cdot \underline{p} + \text{grad } u = 0 \quad \text{on } \Omega, \quad (3.1a)$$

$$\text{div } \underline{p} + bu = f \quad \text{on } \Omega. \quad (3.1b)$$

Notice that we could have used (1.4) directly instead of (3.1a) but that (3.1a) is definitely preferred for reasons which will be clear later. Eqs. (1.1) are thus replaced by Eqs. (3.1a), (3.1b) with (1.1b) and the unknowns are now  $\underline{p}$  and  $u$ . Introducing the space

$$H(\text{div}; \Omega) = \{ \underline{p} \mid \underline{p} \in L^2(\Omega) \times L^2(\Omega), \text{div } \underline{p} \in L^2(\Omega) \}, \quad (3.2)$$

the classical mixed variational formulation of (1.1) written in the above form is then to find  $(\underline{p}, u) \in H(\text{div}; \Omega) \times L^2(\Omega)$  such that

$$\int_{\Omega} \underline{c} \cdot \underline{p} \cdot \underline{q} \, dx - \int_{\Omega} u \, \text{div } \underline{q} \, dx = 0, \quad \forall \underline{q} \in H(\text{div}; \Omega), \quad (3.3a)$$

$$- \int_{\Omega} v \, \text{div } \underline{p} \, dx - \int_{\Omega} b \, uv \, dx = - \int_{\Omega} f v \, dx, \quad \forall v \in L^2(\Omega). \quad (3.3b)$$

The classical discretization of  $H(\text{div}; \Omega)$  is due to Raviart and Thomas <sup>8</sup> in 2D and Nédélec <sup>9</sup> in 3D. In 2D, the Raviart-Thomas spaces constitute a conforming finite element

approximation of  $H(\text{div}; \Omega)$ . Over a rectangular mesh  $(K=\hat{C})$ , the Raviart-Thomas space of index  $k \in \mathbb{N}$  is defined by

$$\begin{aligned} S = R^k(K) &:= Q^{k+1,k} \times Q^{k,k+1} \quad \text{on } K, \\ \dim R^k(K) &= 2(k+1)(k+2), \end{aligned} \quad (3.4a)$$

$$\begin{aligned} D = \mathcal{D}R^k(K) &:= \{ m_H^i(p_{1h}), \quad i=0, \dots, k, \\ &\quad m_C^{ij}(p_{1h}), \quad i=0, \dots, k-1; \quad j=0, \dots, k, \\ &\quad m_V^i(p_{2h}), \quad i=0, \dots, k, \\ &\quad m_C^{ij}(p_{2h}), \quad i=0, \dots, k, \quad j=0, \dots, k-1 \} \quad \text{on } K, \\ \text{card } \mathcal{D}R^k(K) &= 2(k+1)(k+2), \end{aligned} \quad (3.4b)$$

where  $m_H^i$  (resp.  $m_V^i$ ) stands for  $m_L^i$  and  $m_R^i$  (resp.  $m_B^i$  and  $m_T^i$ ),  $\tilde{n}$  is some unit normal to  $\partial C$  and  $\tilde{p}_h = (p_{1h}, p_{2h})$ . Instead of choosing as parameters  $\tilde{p}_h \cdot \tilde{n}$  at some (Gaussian) points on  $\partial C$  as in Ref. 8, we preferred to use moments as in Ref. 9, and we modified slightly their definition in accordance with the normalization adopted in Eqs. (2.3).

Let us now introduce a (conforming) finite element approximation of  $L^2(\Omega)$  over the same mesh and for any  $k \in \mathbb{N}$  by

$$S = Q^k(K), \quad \dim Q^k(K) = (k+1)^2 \quad (3.5a)$$

$$\begin{aligned} D = \mathcal{D}Q^k(K) &:= \{ m_C^{ij}(u_h), \quad i, j=0, \dots, k \} \quad \text{on } K, \\ \text{card } \mathcal{D}Q^k(K) &= (k+1)^2. \end{aligned} \quad (3.5b)$$



Finally, define the following spaces

$$R_{-1}^k(R_h) = \left\{ \underset{\sim}{v} \mid \underset{\sim}{v} \in L^2(\Omega) \times L^2(\Omega) , \right. \\ \left. \underset{\sim}{v} \Big|_K \in R^k(K) , \forall K \in R_h \right\} , \quad (3.6)$$

$$R_0^k(R_h) = \left\{ \underset{\sim}{v} \mid \underset{\sim}{v} \in R_{-1}^k(R_h) , \right. \\ \left. \underset{\sim}{v} \cdot \underset{\sim}{n} \text{ is } \underline{\text{continuous across the interelement}} \right. \\ \left. \underline{\text{boundaries}} \right\} . \quad (3.7)$$

The continuity condition transforming  $R_{-1}^k(R_h)$  into  $R_0^k(R_h)$  which is a conforming approximation of  $H(\text{div}; \Omega)$  can be expressed equivalently by imposing the continuity of the moments  $m_L^i, \dots, m_T^i$  ,  $i=0, \dots, k$  of  $\underset{\sim}{v} \cdot \underset{\sim}{n}$  across the interfaces between different cells.

The classical RTN (for Raviart-Thomas-Nédélec) discretization of problem (3.3) consists in looking for

$(\underset{\sim}{p}_h, \underset{\sim}{u}_h) \in R_0^k(R_h) \times U_{-1}^k(R_h) \subset H(\text{div}; \Omega) \times L^2(\Omega)$  satisfying

$$\int_{\Omega} \underset{\sim}{c} \cdot \underset{\sim}{p}_h \cdot \underset{\sim}{q}_h \, dx - \int_{\Omega} \underset{\sim}{u}_h \, \text{div} \, \underset{\sim}{q}_h \, dx = 0 , \forall \underset{\sim}{q}_h \in R_0^k(R_h) , \quad (3.8a)$$

$$- \int_{\Omega} \underset{\sim}{v}_h \, \text{div} \, \underset{\sim}{p}_h \, dx - \int_{\Omega} b \, \underset{\sim}{u}_h \, \underset{\sim}{v}_h \, dx = - \int_{\Omega} f \, \underset{\sim}{v}_h \, dx , \forall \underset{\sim}{v}_h \in U_{-1}^k(R_h) . \quad (3.8b)$$

The idea here is thus to approximate  $u$  and  $p$  simultaneously, instead of obtaining  $p_h$  by differentiation of  $u_h$  (an operation where one order of convergence is lost) and multiplication by an eventually rough tensor  $a$ . The finite dimensional subspaces  $W_h$  of  $H(\text{div}; \Omega)$  and  $V_h$  of  $L^2(\Omega)$  used need to satisfy certain properties for the convergence analyses of Raviart and Thomas<sup>8</sup>, Falk and Osborn<sup>12</sup> or Douglas and Roberts<sup>13</sup> to hold. One of them is that  $\text{div } W_h \subset V_h$ , clearly satisfied by  $R_0^k$  and  $U_{-1}^k$  and under which the following results<sup>7</sup> are known:

THEOREM 3. For any  $k \geq 0$ , problem (3.8) has a unique solution. Moreover there exists a constant  $C > 0$ , independent of  $h$ , such that

$$\|p - p_h\|_0 \leq C |h|^{k+1} \|p\|_{k+1}, \quad (3.9a)$$

$$\|u - u_h\|_0 \leq C |h|^{k+1} \|u\|_{r-1}, \quad (3.9b)$$

$$\|P_h^k u - u_h\|_0 \leq C |h|^{k+2} \|u\|_r, \quad (3.9c)$$

where  $r = \max(k+2, 3)$ ,  $|h|$  denotes the maximum diameter of the cells of  $R_h$  while  $P_h^k$  is the orthogonal projection of  $L^2$  onto  $U_{-1}^k(R_h)$ .

In the rectangular case and with the choice of parameters made in (3.4b) and (3.5b), it is particularly easy to exhibit explicit and compact expressions for the corresponding basis functions. Corresponding to the degrees of freedom  $m_L^i$ ,  $m_R^i$  and  $m_C^{ij}$  of  $p_{1h}$ , we have the following basis functions

$$p_{1L}^i(x,y) = \frac{1}{2}(-1)^k [P_k(x) - P_{k+1}(x)] P_i(y) , i=0,\dots,k , (3.10a)$$

$$p_{1R}^i(x,y) = \frac{1}{2} [P_k(x) + P_{k+1}(x)] P_i(y) , i=0,\dots,k , (3.10b)$$

$$p_{1C}^{ij}(x,y) = P_{ij}(x,y) - P_{k-1+m(i)}(x)P_j(y) , i=0,\dots,k-1, \\ j=0,\dots,k , (3.10c)$$

where  $m(i)=1$  or  $2$  such that  $i$  and  $k-1+m(i)$  have the same parity. Similar expressions hold for the corresponding degrees of freedom of  $p_2$ , with the roles of  $x$  and  $y$  exchanged and  $L, R$  replaced by  $B, T$ . For the degrees of freedom  $m_C^{ij}$  of  $u_h$ , the basis functions are much simpler and reduce to

$$u_C^{ij}(x,y) = P_{ij}(x,y) , i,j=0,\dots,k , (3.11)$$

The main problem with the mixed element formulation is that it normally leads to linear systems of the form

$$\begin{cases} A\tilde{p}_h + Bu_h = 0 \\ B\tilde{p}_h^T + Cu_h = f \end{cases} , (3.12)$$

which are generally indefinite (if  $b \equiv 0$  so that  $C \equiv 0$ ). This is clearly the case in oil reservoir simulation applications. In numerical reactor calculations on the other hand,  $b$  is in general positive everywhere and such complications do not appear<sup>14</sup>. Recently, Arnold and Brezzi<sup>7</sup> have shown how these problems

could be avoided by the use of the so-called mixed-hybrid formula-  
tion, whereby the continuity constraints upon  $\underline{p}_h \cdot \underline{n}$  inherent to  
the conformity conditions in  $H(\text{div}; \Omega)$  are relaxed and enforced  
instead through Lagrange multipliers defined on the interelement  
boundaries ( $R_{-1}^k(R_h)$  is issued instead of  $R_0^k(R_h)$ ).

To introduce these Lagrange multipliers, we shall need some  
further notation. Let  $E_h$  denote the set of edges  $E$  or rectangles  
in  $R_h$ , which do not belong to the boundary  $\Gamma$  of  $\Omega$ . The space of  
Lagrange multipliers we shall use is the space  $M_{-1}^k(E_h)$  of all  
functions on  $UE$  which restrict to polynomials of degree at most  
 $k$  on each  $E \in E_h$  (and vanish on the edges belonging to  $\Gamma$ ). On our  
rectangular mesh, the multipliers space  $M_{-1}^k(E_h)$  is defined as  
follows

$$\begin{aligned} M_{-1}^k(E_h) &= \{\mu(x \text{ or } y) \mid \mu \in L^2(E_h) \text{ ,} \\ &\quad \mu|_E \in P^k(E) \text{ , } \forall E \in E_h \} \text{ ,} \end{aligned} \quad (3.13)$$

where for any index  $k \in \mathbb{N}$

$$\begin{aligned} S = M^k(E) &:= P^k \text{ on } E \text{ ,} \\ \dim M^k(E) &= k+1 \text{ ,} \end{aligned} \quad (3.14a)$$

$$\begin{aligned} D = \mathcal{DM}^k(E) &:= m_H^i \text{ or } v(\mu_h) \text{ , } i=0, \dots, k \text{ on } E \text{ ,} \\ \text{card } \mathcal{DM}^k(E) &= k+1 \text{ ,} \end{aligned} \quad (3.14b)$$

where the moments of the  $\mu_h$  are horizontal or vertical depending on the orientation of the edge  $E$ . With the normalization (2.3b), the corresponding basis functions are simply  $P_i(x \text{ or } y)$ ,  $i=0, \dots, k$ .

The mixed-hybrid formulation of our original problem can now be defined as follows:

$$\text{Find } (\underline{p}_h, u_h, \underline{\mu}_h) \in R_{-1}^k(R_h) \times U_{-1}^k(R_h) \times M_{-1}^k(\mathcal{E}_h)$$

such that

$$\int_{\Omega} \underline{c} \cdot \underline{p}_h \cdot \underline{q}_h \, dx - \sum_C \left\{ \int_{\Omega} u_h \operatorname{div} \underline{q}_h \, dx - \int_{\partial C} \underline{\mu}_h \cdot \underline{q}_h \, ds \right\} = 0, \quad \forall \underline{q}_h \in R_{-1}^k(R_h), \quad (3.15a)$$

$$- \sum_C \int_C v_h \operatorname{div} \underline{p}_h \, dx - \int_{\Omega} b v_h u_h \, dx = - \int_{\Omega} v_h f \, dx, \quad \forall v_h \in U_{-1}^k(R_h), \quad (3.15b)$$

and

$$\sum_C \int_{\partial C} v_h \underline{p}_h \cdot ds = 0, \quad \forall v_h \in M_{-1}^k(R_h), \quad (3.15c)$$

which gives rise to an algebraic system of the form

$$\begin{cases} \bar{A} \underline{p}_h^* + \bar{B} u_h^* + \bar{C} \mu_h = 0 \\ \bar{B}^T \underline{p}_h^* + \bar{D} u_h^* = f \\ \bar{C}^T \underline{p}_h^* = 0 \end{cases}, \quad (3.16)$$

Arnold and Brezzi <sup>7</sup> proved that (3.16) has a unique solution  $(\underline{p}_h^*, u_h^*, \mu_h)$  and that moreover  $\underline{p}_h^* \equiv \underline{p}_h$  and  $u_h^* \equiv u_h$  where  $(\underline{p}_h, u_h)$  is the unique solution of (3.8). The identity symbol  $\equiv$  here means that corresponding components are identical even if the discrete vectors have different sizes ( $\dim \underline{p}_h^* > \dim \underline{p}_h$  whereas  $\dim u_h^* = \dim u_h$ ). The advantage of (3.16) is that  $\bar{A}$  is block-diagonal, each block corresponding to the flux unknowns in a single element. It is therefore trivial to invert  $\bar{A}$  elementwise to get

$$\underline{p}_h^* = -\bar{A}^{-1} (\bar{B} u_h^* + \bar{C} \mu_h), \quad (3.17)$$

so that (3.16) becomes

$$\begin{cases} (\bar{B}^T \bar{A}^{-1} \bar{B} - \bar{D}) u_h^* + \bar{B}^T \bar{A}^{-1} \bar{C} \mu_h = -f \\ \bar{C}^T \bar{A}^{-1} \bar{B} u_h^* + \bar{C}^T \bar{A}^{-1} \bar{C} \mu_h = 0 \end{cases}, \quad (3.18)$$

which can be shown to be symmetric positive definite even if  $b \equiv 0$  ( $\bar{D} \equiv 0$ ).

In fact, the first equation (3.18) can be solved easily for the  $u_h^*$ 's as again the corresponding matrix is block-diagonal

and we finally remain with a coupled system in  $\mu_h$ , which can be greatly simplified if we organize the corresponding unknowns in horizontal and vertical ones, leading quite naturally to iterative schemes of the ADI type. In Figure 1, we show for illustration purpose the structure of the algebraic systems arising with the mixed and mixed-hybrid formulations respectively in a simple 2D case.

#### 4. POSTPROCESSING OF MIXED-HYBRID FORMULATIONS

The postprocessing of the above mixed-hybrid formulation as proposed by Arnold and Brezzi <sup>7</sup> is based on the fact that the Lagrange multipliers do in fact yield additional information on  $u$  which can be combined with the approximation  $u_h \in U_{-1}^k$  to provide an "extension" or "enhancement"  $\tilde{u}_h$  of greater accuracy than  $u_h$ .

With the choice of parameters which we made for several of the spaces introduced earlier, the postprocessing operation is particularly simple. After solving (3.16) for  $p_h, u_h$  and  $\mu_h$ , the pieces of information we have at our disposal are the following ones:  $u_h$  provides us directly with  $(k+1)^2$  cell moments  $m_C^{ij}$ ,  $i, j=0, \dots, k$ , while  $\mu_h$  gives us  $4(k+1)$  edge moments  $m_E^i$ ,  $i=0, \dots, k$ ;  $E=L, R, B, T$ . With these  $(k+1)(k+5)$  moments, it is trivial to build up  $\tilde{u}_h|_C$  in  $N^k(C)$  cell by cell to come up finally with  $\tilde{u}_h \in N_{-1}^k(R_h)$ .

This operation can be formalized by introducing two orthogonal projectors of  $L^2$  onto  $U_{-1}^k(R_h)$  and  $M_{-1}^k(E_h)$ , namely  $P_h^k$  and  $\Pi_h^k$ : then  $\tilde{u}_h$  is the unique element of  $N_{-1}^k(R_h)$  such that

$$\begin{aligned} P_h^k \tilde{u}_h &= u_h, \\ \Pi_h^k \tilde{u}_h &= \mu_h. \end{aligned} \tag{4.1}$$



Needless to say, this postprocessing operation does not cost anything with our choice of parameters, since knowing the  $(k+1)(k+5)$  edge and cell moments of  $\tilde{u}_h$  yields us directly  $\tilde{u}_h$ .

The fact that  $\tilde{u}_h$  converges to  $u$  faster than  $u_h$  is reflected by

THEOREM 4. Let  $u$  be the solution of (1.1) and  $(p_h, u_h, u_h)$  the solution of the mixed-hybrid discretization (3.15). Define moreover  $\tilde{u}_h \in N_{-1}^k(R_h)$  by (4.1). Then

$$\|u - \tilde{u}_h\|_0 \leq C |h|^{k+2} (\|u\|_r + \|\tilde{p}\|_{k+1}) \quad , \quad r = \max(k+2, 3) \quad , \quad (4.2)$$

with  $C$  independent of  $u$  and  $h$ .

Proof:

As in Arnold and Brezzi <sup>7</sup>, let us introduce  $\tilde{u}_h^* \in N_{-1}^k(R_h)$ , the nonconforming interpolant of  $u$  such that

$$p_h^k(u - \tilde{u}_h^*) = 0 \quad ,$$

and

$$\Pi_h^k(u - \tilde{u}_h^*) = 0 \quad . \quad (4.3)$$

$\tilde{u}_h^*$  clearly exists and is unique. Standard approximation arguments using (2.7) lead moreover to

$$\|u - \tilde{u}_h^*\|_0 \leq C_1 |h|^{k+3-\delta_{k0}} \|u\|_{k+3-\delta_{k0}} \quad (4.4)$$

Combining (4.1) and (4.3), we get

$$P_h^k(\tilde{u}_h^* - \tilde{u}_h) = P_h^k u - u_h \quad ,$$

and

$$\Pi_h^k(\tilde{u}_h^* - \tilde{u}_h) = \Pi_h^k u - \mu_h \quad . \quad (4.5)$$

A simple scaling argument leads then to

$$\|\tilde{u}_h^* - \tilde{u}_h\|_{0,C} \leq C_2 (\|P_h^k u - u_h\|_{0,C} + h^{1/2} \sum_E \| \Pi_h^k u - \mu_h \|_{0,E}) \quad , \quad (4.6)$$

and we need a last technical result (Eq. (1.21) of Theorem 1.4 by Arnold and Brezzi <sup>7</sup>), namely that

$$\|\Pi_h^k u - \mu_h\|_{0,E} \leq C_3 (h^{1/2} \|p - p_h\|_{0,C} + h^{1/2} \|P_h^k u - u_h\|_{0,C}) \quad . \quad (4.7)$$

Then with

$$\|u - \tilde{u}_h\|_0 \leq \|u - \tilde{u}_h^*\|_0 + \|\tilde{u}_h^* - \tilde{u}_h\|_{0,C} \quad , \quad (4.8)$$

(4.2) is easily proved by combining (4.4), (4.6), (4.7) with (3.9a) and (3.9c).

Before leaving this section, a last comment seems to be of order. The convergence rate to  $u$  has been increased as we have seen by one when we build up  $u_h$  from  $\tilde{u}_h$  and  $\mu_h$ , a cost free operation with our selection of parameters. This enhancement of  $u_h$  is essentially due to (3.9c) (and not to (3.9b)). (3.9c) is in fact a superconvergence result for  $u_h$  saying that convergence of  $O(h^{k+2})$  is valid at the  $(k+1) \times (k+1)$  Gauss points, while only  $O(h^{k+1})$  is felt in  $L^2$  norm.

## 5. RELATIONSHIPS WITH DIRECT IMPLEMENTATIONS OF NODAL SCHEMES

After showing in the last section how a trivial postprocessing operation could lead us easily to a more rapidly convergent approximation  $\tilde{u}_h$  to  $u$ , it is interesting to try to relate this approximation  $\in N_{-1}^k(R_h)$  to more direct implementations of nodal schemes. That is what we plan to do in this section.

Let us go back to the mixed-hybrid equations (3.15) and replace  $u_h$  and  $\mu_h$  by  $P_h^k \tilde{u}_h$  and  $\Pi_h^k \tilde{u}_h$  following (4.1). Eq. (3.15a) leads to

$$\int_{\Omega} \underline{c} \cdot \underline{p}_h \cdot \underline{q}_h dx - \sum_C \left\{ \int_C P_h^k \tilde{u}_h \operatorname{div} \underline{q}_h dx - \int_{\partial C} \Pi_h^k \tilde{u}_h \underline{q}_h \cdot \underline{n} ds \right\} = 0$$

$$\forall \underline{q}_h \in R_{-1}^k(R_h), \quad (5.1)$$

or after expressing  $\tilde{u}_h$  as  $P_h^k \tilde{u}_h + (I - P_h^k) \tilde{u}_h$ , where  $(I - P_h^k) \tilde{u}_h$  is orthogonal to  $\operatorname{div} \underline{q}_h \in C U_{-1}^k(R_h)$ , we finally get

$$\int_{\Omega} \underline{c} \cdot \underline{p}_h \cdot \underline{q}_h dx - \sum_C \left\{ \int_C \tilde{u}_h \operatorname{div} \underline{q}_h dx - \int_{\partial C} \Pi_h^k \tilde{u}_h \underline{q}_h \cdot \underline{n} ds \right\} = 0$$

$$\forall \underline{q}_h \in R_{-1}^k(R_h), \quad (5.2)$$

which after integration by parts of the  $\int_C$  terms leads to

$$\int_{\Omega} \underline{c} \cdot \underline{p}_h \cdot \underline{q}_h dx + \sum_C \int_C \underline{q}_h \cdot \operatorname{grad} \tilde{u}_h dx = 0, \quad \forall \underline{q}_h \in R_{-1}^k(R_h), \quad (5.3)$$

A similar operation with Eq. (3.15b) successively leads to

$$-\sum_C \int_C v_h \operatorname{div} \underline{p}_h dx - \int_{\Omega} v_h (bu_h - f) dx = 0, \quad \forall v_h \in U_{-1}^k(R_h), \quad (5.4)$$

or with  $P_h^k \tilde{v}_h = v_h$  and  $\tilde{v}_h = P_h^k \tilde{v}_h + (I - P_h^k) \tilde{v}_h$ , where the last term is orthogonal to  $\operatorname{div} \underline{p}_h$  to

$$-\sum_C \int_{\partial C} \tilde{v}_h \underline{p}_h \cdot ds + \sum_C \int_C \underline{p}_h \cdot \operatorname{grad} \tilde{v}_h dx - \int_{\Omega} v_h (bu_h - f) dx = 0, \quad \forall v_h \in U_{-1}^k(R_h), \quad (5.5)$$

or taking into account (3.15c) to

$$\sum_C \int_C \underline{p}_h \cdot \operatorname{grad} \tilde{v}_h dx - \int_{\Omega} v_h (bu_h - f) dx = 0, \quad \forall v_h \in U_{-1}^k(R_h), \quad (5.6)$$

which can be replaced by

$$\sum_C \int_C \underline{p}_h \cdot \operatorname{grad} \tilde{v}_h dx - \int_{\Omega} \tilde{v}_h P_h^k (bu_h - f) dx = 0, \quad \forall v_h \in U_{-1}^k(R_h), \quad (5.7)$$

provided  $(bu_h - f)$  is replaced by its  $L^2$  orthogonal projection onto  $U_{-1}^k(R_h)$ . The final equations are thus

$$\int_{\Omega} \underline{c} \underline{p}_h \cdot \underline{q}_h dx + \sum_C \int_C \underline{q}_h \cdot \text{grad } \tilde{u}_h dx = 0, \quad \forall \underline{q}_h \in R_{-1}^k(R_h), \quad (5.8a)$$

and

$$\sum_C \int_C \underline{p}_h \cdot \text{grad } \tilde{v}_h dx - \int_{\Omega} \tilde{v}_h P_h^k (v u_h - f) dx = 0, \quad \forall \tilde{v}_h \in N_{-1}^k(R_h), \quad (5.8b)$$

Let us first assume as in Arnold and Brezzi <sup>7</sup> that  $\underline{c}$  is of the form  $c_{ij} = c(x) \delta_{ij}$ , where  $c$  is piecewise constant, and constant in particular on each  $C \in \mathcal{R}_h$ . Eq. (5.8a) then means that  $\underline{c} \underline{p}_h$  is the  $L^2$  projection of  $-\text{grad } \tilde{u}_h$  onto  $R_{-1}^k(R_h)$ , or denoting by  $Q_h^k$  this projection operator

$$\underline{c} \underline{p}_h = - Q_h^k (\text{grad } \tilde{u}_h), \quad (5.9)$$

and since  $\underline{c} := \underline{a}^{-1}$ , (5.8b) becomes

$$\sum_C \int_C \underline{a} Q_h^k (\text{grad } \tilde{u}_h) \cdot \text{grad } \tilde{v}_h dx + \int_{\Omega} P_h^k (b u_h - f) \tilde{v}_h dx = 0, \quad \forall \tilde{v}_h \in N_{-1}^k(R_h). \quad (5.10)$$

In many practical applications (see Ref. 14 for instance),  $b$  is also piecewise constant, so that (5.10) can be rewritten as

$$\sum_C \int_C \underline{a} Q_h^k(\text{grad } \tilde{u}_h) \cdot \text{grad } \tilde{v}_h dx + \int_{\Omega} (b P_h^k \tilde{u}_h - P_h^k f) \tilde{v}_h dx = 0, \quad \forall \tilde{v}_h \in N_{-1}^k(R_h) \quad (5.11)$$

Solving the mixed-hybrid equations (3.15) for  $(p_h, u_h, \mu_h)$  and building up the enhancement  $\tilde{u}_h$  of  $u_h$  from the data  $u_h$  and  $\mu_h$  is thus equivalent to find  $\tilde{u}_h \in N_{-1}^k(R_h)$  such that (5.11) be satisfied for all  $\tilde{v}_h \in N_{-1}^k(R_h)$ . As  $N_{-1}^k(R_h) \not\subset H_0^1(\Omega)$ , this is in fact a primal nonconforming finite element formulation of the original problem (1.1) within the nodal space  $N_{-1}^k(R_h)$ , which exhibits two nonstandard features:

a. the gradient of  $\tilde{u}_h$  is projected onto  $R_{-1}^k(R_h)$ ,

and

b. in the mass-like terms, a projection onto  $U_{-1}^k(R_h)$  appears.

In many important applications,  $f$  is replaced by its nonconforming interpolant  $\tilde{f}_h^* \in N_{-1}^k(R_h)$  such that

$$P_h^k(f - \tilde{f}_h^*) = 0$$

and

$$\Pi_h^k(f - \tilde{f}_h^*) = 0 \quad (5.12)$$

Consequently, the projection of the mass-like terms onto  $U_{-1}^k(R_h)$  is from  $N_{-1}^k(R_h)$  only: as mentioned in Theorem 2, this is exactly what the Radau quadrature does to the mass-like terms, and to them only since it does not affect the stiffness-like terms. In other words, the enhanced RTN mixed-hybrid approximation is clearly related to the p.n.m. (and not to the m.n.m.). In 1D applications, where  $Q_h^k \equiv I$  (and where the nonconforming aspect disappears by the way), we have reported elsewhere <sup>14</sup> calculations where clearly the enhanced mixed-hybrid results is identical to the result obtained directly with the primal p.n.m. The other nonstandard feature is the projection of  $\text{grad } \tilde{u}_h$  onto  $R_{-1}^k(R_h)$ : this operation only appears in multidimensional calculations. In 2D for instance,

$$\text{grad } \tilde{u}_h \subset (Q_{k+1,k} \cup Q_{k-1,k+2}) \times (Q_{k+2,k-1} \cup Q_{k,k+1})$$

$$\forall \tilde{u}_h \in N_{-1}^k, \text{ if } k > 0, \quad (5.13a)$$

or

$$\text{grad } \tilde{u}_h \subset Q_{1,0} \times Q_{0,1} \equiv R_{-1}^0(R_h)$$

$$\forall \tilde{u}_h \in N_{-1}^0, \text{ if } k = 0. \quad (5.13b)$$

Except for  $k=0$ ,  $\text{grad } \tilde{u}_h \not\subset R_{-1}^k$  and the projection is required.



As we shall see below, this projection can be related to an operation well-known by the nuclear engineers who developed the first nodal schemes, namely the transverse integration leading to dimensionally reduced nodal schemes. See e.g. Ref. 1 or Section 5 of Ref. 3. The basic idea is to proceed to some transverse averaging of the given equation in all dimensions minus one, in order to stay with only 1D equations. In 2D, for instance the original equation (1.1a) with  $\underline{a}:=a(x)\delta_{ij}$  is successively multiplied by  $p_{jl}(y)$ ,  $l=0,\dots,k$  and integrated in the  $y$  direction between  $y_{Bj}$  and  $y_{Tj}$ ,  $j=1,\dots,J$  as  $\Omega$  is divided into  $J$  horizontal slices,  $p_{jl}(y)$  being the modified 1' the Legendre polynomial

$$p_{jl}(y) = P_l \left\{ \frac{2(y-y_j)}{y_{Tj}-y_{Bj}} \right\}, \quad (5.14)$$

where the notation is that of Figure 2. The same operation is then performed in the  $x$  direction between  $x_{Li}$  and  $x_{Ri}$ ,  $i=1,\dots,I$  after multiplication by  $p_{il}(x)$ ,  $l=0,\dots,k$ . The result of the transverse integration procedure is a set of  $2(k+1)$ ,  $N(k+1)$  in  $\mathbb{R}^N$ , one-dimensional equations, namely

$$-a \frac{d^2 u_{xj}^1(x)}{dx^2} + bu_{xj}^1(x) = \hat{f}_{xj}^1(x) \quad , \quad l=0, \dots, k \quad , \quad (5.15a)$$

$$-a \frac{d^2 u_{iy}^1(y)}{dy^2} + bu_{iy}^1(y) = \hat{f}_{iy}^1(y) \quad , \quad l=0, \dots, k \quad , \quad (5.15b)$$

where  $a$  and  $b$  have been assumed constant for the sake of simplicity and where

$$u_{xj}^1(x) = \frac{\int_{y_{Bj}}^{y_{Tj}} p_{jl}(y) u(x, y) dy}{\int_{y_{Bj}}^{y_{Tj}} p_{jl}^2(x) dy} \quad , \quad l=0, \dots, k \quad , \quad (5.16a)$$

$$u_{iy}^1(x) = \frac{\int_{x_{Li}}^{x_{Ri}} p_{jl}(x) u(x, y) dx}{\int_{x_{Li}}^{x_{Ri}} p_{jl}^2(x) dx} \quad , \quad l=0, \dots, k \quad . \quad (5.16b)$$

In (5.15a) for instance,  $\hat{f}_{xj}^1(x)$  is an effective source term including the 1'th 1D moment of  $f(x, y)$ ,  $f_{xj}^1(x)$  defined analogously to  $u_{xj}^1(x)$ , as well as a transverse leakage term,  $\ell_{xj}^1(x)$ , arising from the cell boundary values of the  $y$  integral of the differential operator with respect to  $y$ . For more details, see Ref. 3.

As such, the transverse integration procedure appears to be no more than a computational trick leading to sets of 1D equations, which will then be solved iteratively in an ADI way. This reduction to 1D problems was especially needed in connection with the so-called analytical nodal methods<sup>1</sup>, where the basis functions were taken to be fundamental solutions of the (1D) equations, plus some particular solutions corresponding to simple second members (polynomials of low degree). These fundamental solutions are easy to find in 1D with piecewise constant  $a$  and  $b$ : they are basically combinations of hyperbolic sines and cosines. This is not so in multidimensional situations.

If we go back to Eqs. (5.15) and put them in a weak form (by multiplication by some test function and integration by parts), it is easy to realize that if  $u$  is looked for in  $N_{-1}^k(R_h)$ , the transverse integrated form projects the gradient of  $u$  onto  $R_{-1}^k(R_h)$ . If moreover, a p.n.m. is used instead of an m.n.m. to solve the resulting 1D equations, the mass-like terms are projected onto  $U_{-1}^k(R_h)$  (while the stiffness-like terms remain unaffected by the corresponding projection operation as it is done under Radau quadrature). The final result is expressed in

THEOREM 5. The enhanced RTN mixed-hybrid approximation to  $u$  is equivalent to the primal nonconforming nodal approximation obtained through physical arguments (the p.n.m.), when moreover transverse integration is used if  $k > 0$ .

Before leaving this Section, we would like to make a few comments. As we have seen in Section 4, it is fairly easy to obtain convergence results for mixed-hybrid approximations, if all what is known about mixed approximations is used. Deriving such convergence rates directly from the nonconforming primal formulation is somewhat more tricky: in a previous paper <sup>3</sup>, we mentioned that rates of  $O(h^{k+2})$  were guaranteed by the fact that  $P^{k+1}$  was included in  $N^k$  in  $C$  on one hand (see (2.7)) and that a patch test of order  $k$  was passed on  $\partial C$  on the other hand. In further papers <sup>4,14</sup>, these convergences rates were proved numerically. Theoretical convergence proofs are given for the first time here: they apply to the physical version under transverse integration, but it is clear that they should be valid also for the mathematical version also, with or without transverse integration, as numerical results do confirm <sup>4,14</sup>.

If the mixed-hybrid implementation is compared to the direct nonconforming one, we have seen in this Section that the mixed-hybrid version is particularly easy to implement as many operations (like determining  $p_h$  and  $u_h$ ) are performed element-wise.

It is fair to say (and we shall mention it in Section 6) that with the use of static condensation techniques, algebraic systems of the same size and structure are finally solved.

If  $p_h$  has some interest in itself (as in oil reservoir simulation problems), it is directly treated in a better way in the mixed-hybrid formulation, but after the enhancement from  $u_h$  to  $\tilde{u}_h$  it is still possible to differentiate the final approximation  $\tilde{u}_h$  to recover a  $\tilde{p}_h$  of the same order of accuracy as  $p_h$ . A net advantage comes from the fact that the matrix elements in the mixed-hybrid formulation are clearly simpler to evaluate as they involve lower degree polynomials than in the direct nonconforming approach. In the case we have examined in detail hereabove with  $\underline{a}$  a diagonal tensor, piecewise constant like  $b$ , the two approaches are strictly equivalent (and do in fact produce the same numerical results <sup>14</sup>). The major interest of the mixed-hybrid implementation comes from the fact that in more general situations it is the only to directly lead to the harmonic average of the eventually rough coefficients in  $\underline{a}$  as we shall discuss in the next Section. More details on the general case, where  $\underline{a}$  and  $b$  are not piecewise constant can be found in Arnold and Brezzi <sup>7</sup>.

## 6. NODAL SCHEMES AND MESH-CENTERED FINITE DIFFERENCES

---

It was shown recently by Russell and Wheeler <sup>15</sup> that using a clever combination of trapezoidal and midpoint quadrature rules the mixed finite element approximation to (1.1) boils down to the corresponding classical mesh-centered finite difference approximation *at the lowest order  $k=0$* . Such a result was later used by M.F. Wheeler and her colleagues to provide a well founded preconditioner for iterative solutions of the mixed finite element algebraic equations resulting from *the lowest order approximation* to the miscible displacement problem in oil reservoir simulation <sup>16,17</sup>.

In this Section, we want to show that a similar result holds for nodal schemes *of any order  $k$* , so that potential preconditioners *of any order  $k$*  can be provided for the corresponding mixed or mixed-hybrid finite element algebraic equations. In principle, when the nodal equations (2.8) in the primal formulation are solved, any finite element expert would be tempted to eliminate the unknowns belonging to only one node, that is the cell moments  $m_C^{ij}$ , by a procedure quite classical known as static condensation, to finally remain with a system of algebraic equations in the edge moments  $m_E^i$  only, quite similar to the system corresponding to the Lagrange multipliers in the mixed-hybrid formulation. In fact as we explain with more details in a forthcoming institutional report <sup>18</sup>, the nuclear engineers

involved in the development of the first nodal schemes <sup>19,20</sup> proposed quite tricky strategies to eliminate instead the edge unknowns in terms of the cell ones, in an attempt to finally get point or block mesh-centered finite difference like algebraic equations. We won't try here to formalize and analyze the approach used, but we refer the interested readers to the original references <sup>19,20</sup> or to the forthcoming report <sup>18</sup>. The main reason behind such "tricks" seems to have been the implicit recognition by the reactor calculation community that the mesh- or block-centered finite differences are in some way superior to the point-centered finite differences, which still seem more favored by the mathematical community (Wachspress' box integration method <sup>21</sup> for instance is point-centered). It is interesting to point out here that the same situation prevails in oil reservoir simulation, where point-centered finite difference schemes are used in a small minority of industrial simulators <sup>15</sup>. The key point is that in presence of rough coefficients the mesh-centered schemes lead to harmonic averaging of  $\underline{a}$ , while the point-centered ones provide an arithmetic averaging of the corresponding tensor. In 1D, the harmonic average is the correct one with rough coefficients. This is no longer the case in more than 1D, but the harmonic averaging is still better than the arithmetic one. At the beginning of Section 3, we briefly mentioned that (3.1a) was preferred to (1.4): This is because (3.1a) directly leads to harmonic averaging, and not (1.4). There is

thus a "good" and a "bad" mixed method and in presence of rough coefficients they yield dramatically different results, as simple numerical experiments show <sup>14,22</sup>.

Let us now proceed to derive mesh-centered finite difference schemes from nodal schemes: our approach will be based on the use of particular numerical quadrature rules, for the stiffness matrix only. For the mass matrix, the Radau quadrature rules will still be used. Assume that the vector  $\underline{u} = [u_1, \dots, u_n]^T$  of basis functions, where  $N=(k+1)(k+5)$  is partitioned following

$$\underline{u} = \begin{bmatrix} \underline{u}_H \\ \underline{u}_C \\ \underline{u}_V \end{bmatrix}, \quad (6.1)$$

where

$$\underline{u}_H = [u_L^0, \dots, u_L^k, u_R^0, \dots, u_R^k]^T,$$

$$\underline{u}_C = [u_C^{00}, u_C^{10}, \dots, u_C^{kk}]^T,$$

and

$$\underline{u}_V = [u_B^0, \dots, u_B^k, u_T^0, \dots, u_T^k]^T. \quad (6.2)$$

Let us introduce the elementary mass and stiffness matrices  $M^e$  and  $K^e$  of order  $N$  as



$$M^e = (m_{ij}^e) \quad ,$$

$$K^e = (k_{ij}^e) = K^{ex} + K^{ey} \quad (6.3)$$

where

$$m_{ij}^e = \int_{-1}^{+1} \int_{-1}^{+1} u_i(x,y) u_j(x,y) dx dy \quad , \quad i,j=1,\dots,N$$

$$k_{ij}^e = \int_{-1}^{+1} \int_{-1}^{+1} \{u_{ix}(x,y) u_{jx}(x,y) + u_{iy}(x,y) u_{jy}(x,y)\} dx dy$$

$$= k_{ij}^{ex} + k_{ij}^{ey} \quad , \quad i,j=1,\dots,N \quad , \quad (6.4)$$

the separation of  $k^e$  in  $k^{ex} + k^{ey}$  being justified by the fact that here again we shall assume  $\underline{a} := a(x)\delta_{ij}$  where  $a(x)$  piecewise constant. As  $M^e$  and  $K^e$  are partitioned according to (6.1), we have for instance

$$M^e = \begin{bmatrix} M_{HH}^e & M_{HC}^e & M_{HV}^e \\ M_{CH}^e & M_{CC}^e & M_{CV}^e \\ M_{VH}^e & M_{VC}^e & M_{VV}^e \end{bmatrix} \quad (6.5)$$

If the matrix elements are evaluated exactly, it is easy to realize that

$$M_{HV}^e = (M_{VH}^e)^T = K_{HV}^e = (K_{VH}^e)^T = 0 \quad , \quad (6.6)$$

so that the coupling between the H (for horizontal) and V (for vertical) components is only via the cell parameters.

Using as above the Radau quadrature rules for the mass matrices reduce them to diagonal matrices, with elements different from zero only in the  $M_{CC}^e$  block: actually

$$(u_C^{ij}, u_C^{kl}) = (P_{ij}, P_{kl}) = \frac{4}{(2i+1)(2j+1)} \delta_{ik} \delta_{il} , \quad (6.7)$$

so that in the particularly simple case  $k=0$ , we shall have

$$M^e = \frac{\Delta x \Delta y}{4} \begin{bmatrix} 0 & 0 & 0 & 0 & 0 \\ 0 & 0 & 0 & 0 & 0 \\ 0 & 0 & 4 & 0 & 0 \\ 0 & 0 & 0 & 0 & 0 \\ 0 & 0 & 0 & 0 & 0 \end{bmatrix} , \quad (6.8)$$

where the scaling factor  $\frac{\Delta x \Delta y}{4}$  takes into account the fact that we consider  $C$  and not the reference cell  $\hat{C} = [-1, +1] \times [-1, +1]$ .

The  $x$  elementary stiffness matrix for instance will have the following structure

$$K^{ex} = \begin{bmatrix} K_{HH}^{ex} & K_{HC}^{ex} & 0 \\ K_{CH}^{ex} & K_{CC}^{ex} & K_{CV}^{ex} \\ 0 & K_{VC}^{ex} & K_{VV}^{ex} \end{bmatrix} , \quad (6.9)$$

and if we want to come up with mesh-centered like finite difference equations we must cancel out the blocks  $K_{CV}^{ex}$ ,  $K_{VC}^{ex}$  and  $K_{VV}^{ex}$ ,

which again is easily done by using a Radau rule in the vertical direction. We also need to eliminate the couplings between the left and right horizontal unknowns: we have for instance

$$(u_{Lx}^i, u_{Rx}^j) \propto \int dy P_i(y) P_j(y) \cdot \int dx (P'_{k+1}(x)^2 - P'_{k+2}(x)^2), \quad (6.10)$$

so that a quadrature rule in the horizontal direction would do the job if it uses as quadrature points the zeros of  $P'_{k+1}(x) \pm P'_{k+2}(x)$ , the cancelation due to a  $\delta_{ij}$  factor being incidental. Considerations of parity show that if  $x_i$  is a zero of  $P'_{k+1} + P'_{k+2}$ ,  $-x_i$  will be a zero of  $P'_{k+1} - P'_{k+2}$  and it is thus sufficient to look for the zeros of  $P'_{k+1} + P'_{k+2}$ . Since

$$P'_{k+1} = (2k+1)P_k + (2k-3)P_{k-2} + (2k-7)P_{k-4} + \dots \quad (6.11a)$$

and

$$P'_{k+2} = (2k+3)P_{k+1} + (2k-1)P_{k-1} + (2k-5)P_{k-3} + \dots, \quad (6.11b)$$

$$P'_{k+1} + P'_{k+2} = \sum_{l=0}^{k+1} (2l+1)P_l. \quad (6.12)$$

For instance

$$\begin{aligned} P'_1 + P'_2 &= P_0 + 3P_1, \\ P'_2 + P'_3 &= P_0 + 3P_1 + 5P_2, \\ P'_3 + P'_4 &= P_0 + 3P_1 + 5P_2 + 7P_3, \end{aligned} \quad (6.13)$$

etc.

$P'_{k+1}$  is a polynomial of degree  $k$  that we shall call  $Q_k$ . The set of polynomials  $Q_k$ ,  $k \in \mathbb{N}$ , is actually a family of orthogonal polynomials over  $[-1, +1]$ , namely ultraspherical polynomials<sup>23</sup> corresponding to the weight  $(1-x^2)$ . Their zeros are in fact the inner (excluding  $\pm 1$ ) points of the Lobatto quadrature formulae. Using Theorem 3.3.4, p.46, of Szegő<sup>23</sup>, it is an easy matter to show that the  $(k+1)$  zeros of  $P'_{k+1} + P'_{k+2} = Q_k + Q_{k+1}$  are real, distinct and that they are in the interior of  $[-1, +1]$ .

Let us give some examples. For  $k=0$ ,  $P'_1 + P'_2 = 1 + 3x$  and the 2  $(2(k+1))$  zeros of  $P'_1 \pm P'_2$  are

$$x_1 = +1/3, \quad x_2 = -1/3, \quad (6.14)$$

the corresponding quadrature rule (exact for linear polynomials) being

$$\int_{-1}^{+1} f(x) dx \approx f(-1/3) + f(+1/3), \quad (6.15)$$

a well-known quadrature rule of the (open) Newton-Cotes type.

For  $k=1$ ,  $P'_2 + P'_3 = P_0 + 3P_1 + 5P_2$  and the 4 real zeros of  $P'_2 \pm P'_3$  are  $\pm a$  and  $\pm b$  with

$$a = (1 + \sqrt{6})/5, \quad b = (-1 + \sqrt{6})/5, \quad (6.16)$$

the corresponding quadrature rule being

$$\int_{-1}^{+1} f(x) dx \approx w_a [f(-a) + f(a)] + w_b [f(-b) + f(b)] \quad , \quad (6.17)$$

with

$$w_a = (3\sqrt{6}+2)/6\sqrt{6} \quad , \quad w_b = (3\sqrt{6}-2)/6\sqrt{6} \quad , \quad (6.18)$$

exact for polynomials of degree less than or equal to three, etc.

In the case  $k=0$ , the elementary stiffness matrices will become under such quadrature rule (product of Radau by open Newton-Cotes here)

$$K^{ex} = \frac{\Delta y}{\Delta x} \begin{bmatrix} 2 & 0 & -2 & 0 & 0 \\ 0 & 2 & -2 & 0 & 0 \\ -2 & -2 & 4 & 0 & 0 \\ 0 & 0 & 0 & 0 & 0 \\ 0 & 0 & 0 & 0 & 0 \end{bmatrix} \quad , \quad (6.19a)$$

and

$$K^{ey} = \frac{\Delta x}{\Delta y} \begin{bmatrix} 0 & 0 & 0 & 0 & 0 \\ 0 & 0 & 0 & 0 & 0 \\ 0 & 0 & 4 & -2 & -2 \\ 0 & 0 & -2 & 2 & 0 \\ 0 & 0 & -2 & 0 & 2 \end{bmatrix} \quad , \quad (6.19b)$$

We shall now prove that these stiffness matrices and the mass matrix (6.8) lead to the classical mesh-centered finite difference scheme. We shall use the notation of Figure 3, where intentionally the mesh is nonuniform and where the mean edge and cell values are conventionally associated with the corresponding centers of gravity. Let us first look at the equation for  $u_R$ : this equation comes from the assembly of two elementary matrices corresponding to cell 0 and cell E. Since the Radau quadrature associates no mass to the edge parameters and because of the cancellation of the couplings of  $u_{Rx}$  with  $u_{Lx}$  (by Newton-Cotes quadrature) and with  $u_{Bx}$  and  $u_{Tx}$  (by Radau quadrature in general; for  $k=0$  these contributions are always zero), the final equation is a relationship between  $u_0$ ,  $u_R$  and  $u_E$ , namely

$$a_0 \frac{\Delta y_0}{\Delta x_0} (2u_R - 2u_0) + a_E \frac{\Delta y_0}{\Delta x_E} (2u_R - 2u_E) = 0, \quad (6.20)$$

which allows us to eliminate  $u_R$  in function of  $u_0$  and  $u_E$ :

$$u_R = \frac{a_0 u_0 / \Delta x_0 + a_E u_E / \Delta x_E}{a_0 / \Delta x_0 + a_E / \Delta x_E}. \quad (6.21)$$

The equation in  $u_0$  on the other hand reads

$$\begin{aligned}
 & a_0 \frac{\Delta y}{\Delta x_0} (-2u_L - 2u_R + 4u_0) \\
 & + a_0 \frac{\Delta x}{\Delta y_0} (-2u_B - 2u_T + 4u_0) \\
 & + b_0 \Delta x_0 \Delta y_0 u_0 = f_0 \Delta x_0 \Delta y_0
 \end{aligned} \tag{6.22}$$

The  $b$  and  $f$  terms are classical with mesh-centered finite differences and we realize that using (6.21) and similar expressions for  $u_L$ ,  $u_B$  and  $u_T$ , we would finally come up with an expression relating  $u_0$  to its four closest neighbors,  $u_W$ ,  $u_E$ ,  $u_S$  and  $u_N$ , namely a five-points difference scheme. To check that this expression is well the mesh-centered one, we must look closer at for instance the terms corresponding to the leakage to the right of cell 0 and show that they are well written as

$$- \Delta y_0 a_R \frac{u_E - u_0}{R}, \tag{6.23}$$

where  $R = (\Delta x_0 + \Delta x_E)/2$  while  $a_R$  is the harmonic average given by

$$a_R = \frac{\Delta x_0 + \Delta x_E}{\Delta x_0 / a_0 + \Delta x_E / a_E} \tag{6.24}$$

These leakage terms come from the first term of (6.22) where all the  $u_R$  and half of the  $u_0$  contributions are considered. Using (6.21), it is a simple matter then to check that these terms do yield (6.23) so that the five points mesh-centered finite differences are well recovered.

The interest of this result consists in the fact that as in the case of the lowest order mixed method examined by M.F. Wheeler and her colleagues a good preconditioner for solving the corresponding algebraic systems is at hand. Here moreover, we dispose of a general technique for building up such preconditioners for any  $k$ , and not only for  $k=0$ . The use of the product integration rules with  $2(k+1)$  fixed points (the zeros of  $P'_{k+1} \pm P'_{k+2}$ ) in one direction ( $x$  for  $K^{ex}$  or  $y$  for  $K^{ey}$ ) and  $k+2$  Radau points in the other direction, combined with a fully  $(k+2) \times (k+2)$  quadrature rule for the mass-like terms, leads to quadrature schemes which reproduce all the polynomials belonging to  $Q^{2k+1, 2k+2}$  or  $Q^{2k+2, 2k+1} \supset Q^{2k+1}$ , and are therefore consistent with the accuracy expected from the underlying nodal schemes (of  $O(h^{k+2})$ ). In each case, (i.e. for any  $k \in \mathbb{N}$ ), the result is a mesh-centered finite difference like scheme of the 5-point type if  $k=0$ , and in general of the 5-block type for  $k > 0$ . In the lowest order case, we keep second order accuracy, because after all the underlying polynomial space includes  $P^1$  cell by cell and has zeroth order moments continuous through the faces of the cell. In the mesh-centered finite differences examined by M.F. Wheeler and her colleagues, the underlying approximation is the lowest order mixed one with  $u$  piecewise constant and first order is expected, with second order only at the centers of gravity of the nodes, a superconvergence result induced by (3.9c). More details about the higher order finite difference scheme ( $k > 0$ ) mentioned hereabove will be found elsewhere <sup>18, 25</sup>



#### ACKNOWLEDGEMENT

This research was supported in part by the "Institut National de Recherche en Informatique et en Automatique" (INRIA) in Rocquencourt, France, where the author spent a few months during the spring of 1984. It was otherwise supported by the IBM Corporation Scientific Centers in Palo Alto, California and Mexico City, Mexico, as well as by the Mexican "Consejo Nacional de Ciencia y Tecnología" (CONACyT).

## REFERENCES

---

1. DORNING, J.J., Modern coarse-mesh methods. A development of the '70's. pp.3.1-3.31 of *Computational Methods in Nuclear Engineering*. American Nuclear Society, Williamsburg, Virginia, (1979).
2. FEDON MAGNAUD, C., HENNART, J.P., and LAUTARD, J.J., On the relationship between some nodal schemes and the finite element method in static diffusion calculations. pp.987-1000 of *Advances in Reactor Computations*. American Nuclear Society, Salt Lake City, Utah, (1983).
3. HENNART, J.P., A general family of nodal schemes. *Com. Tec. Serie NA. 354*, 63 p., IIMAS-UNAM (1983). To appear in *SIAM J. on Scientific and Statistical Computing*.
4. HENNART, J.P., A general finite element framework for nodal methods in *MAFELAP 1984. The Mathematics of Finite Elements and Applications*, J.R. WHITEMAN, Ed., Academic Press, London. To appear.
5. CHAVENT, G., COHEN, G., and JAFFRE, J. Discontinuous upwind ing and mixed finite elements for two-phase flows in reservoir simulation. *Computer methods in Applied Mechanics and Engineering*. To appear.
6. DOUGLAS, Jr., J., EWING, R.E., and WHEELER, M.F., A time-discretization procedure for a mixed finite element approximation of miscible displacement in porous media. *RAIRO Numerical Analysis* 17, 249-265 (1983).
7. ARNOLD, D.N. and BREZZI, F., Mixed and nonconforming finite element methods: implementation, postprocessing and error estimates. *RAIRO Numerical Analysis*. To appear.

8. RAVIART, P.A. and THOMAS, J.M., A mixed finite element method for second order elliptic problems. pp.292-315 of *Mathematical Aspects of the Finite Element Method, Lecture Notes in Mathematics* 606. Springer-Verlag, Heidelberg (1977).
9. NEDELEC, J.C., Mixed finite elements in  $\mathbb{R}^3$ . *Numer. Math.* 35, 315-341 (1980).
10. STRANG, G. and FIX, G.J., *An Analysis of the Finite Element Method*, Prentice Hall, Englewood Cliffs, New Jersey (1973).
11. GLADWELL, I. and WAIT, R., Eds. *A Survey of Numerical Methods for Partial Differential Equations*, Clarendon Press, Oxford (1979).
12. FALK, R.S. and OSBORN, J.E., Error estimates for mixed methods. *RAIRO Numerical Analysis*, 14, 249-277 (1980).
13. DOUGLAS, Jr., J. and ROBERTS, J.E., Global estimates for mixed methods for second order elliptic equations. *Math. Comp.* To appear.
14. DEL VALLE, E., HENNART, J.P., and MEADE, D., Finite element formulations of nodal schemes for neutron diffusion and transport problems in *Advances in Nuclear Engineering Computational Methods*. American Nuclear Society, Knoxville, Tennessee. To appear.
15. RUSSELL, T.E. and WHEELER, M.F., Finite element and finite difference methods for continuous flows in porous media. pp.35-106 of *The Mathematics of Reservoir Simulation*, R.E. EWING, Ed., SIAM, Philadelphia (1983).

16. WHEELER, M.F. and GONZALEZ, R., Mixed finite element methods for some petroleum reservoir engineering problems in *Proceedings Sixth International Conference on Computing Methods in Applied Science and Engineering*, R. GLOWISNKY and J.L. LIONS, Eds., North-Holland, Amsterdam. To appear.
17. WHEELER, M.F. and WEISER, A., Some superconvergence results for a mixed finite element methods in *MAFELAP 1984. The Mathematics of Finite Elements and Applications*, J.R. WHITEMAN, Ed., Academic Press, London. To appear.
18. HENNART, J.P. et al., Advances in numerical reactor calculations. Part I. In preparation.
19. LANGENBUCH, S., MAURER, W., and WERNER, W., Coarse-mesh flux expansion method for the analysis of space-time effects in large light water reactor cores. *Nucl. Sci. and Engng.* 63, 437-456 (1977).
20. LANGENBUCH, S., MAURER, W., and WERNER, W., High-order schemes for neutron kinetics calculations, based on a local polynomial approximation. *Nucl. Sci. and Engng.* 64, 508-516 (1977).
21. WACHSPRESS, E.L., *Iterative Solution of Elliptic Systems and Applications to the Neutron Diffusion Equations of Reactor Physics*, Prentice-Hall, Englewood Cliffs, New Jersey (1966).
22. BABUSKA, I. and OSBORN, J.E., Generalized finite element methods: Their performance and their relation to mixed methods. *SIAM J. Num. Anal.* 20, 510-536 (1983).
23. SZEGÖ, G., *Orthogonal Polynomials*, AMS Colloquium Publications, Volume XXIII, Fourth Edition, American Mathematical Society, Providence, Rhode Island (1975).

24. CIARLET, P.G., *The Finite Element Method for Elliptic Problems*, Exercise 4.1.7., p.204, North-Holland, Amsterdam (1978).
25. HENNART, J.P.. In preparation.

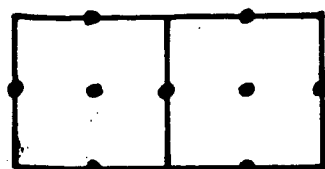
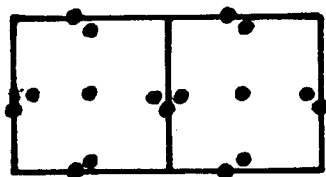
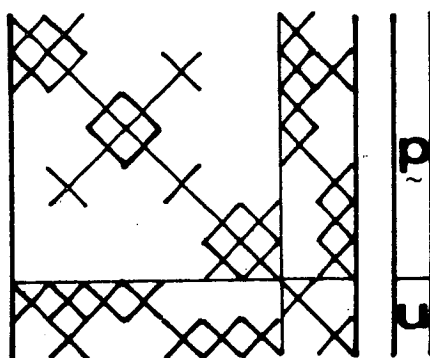
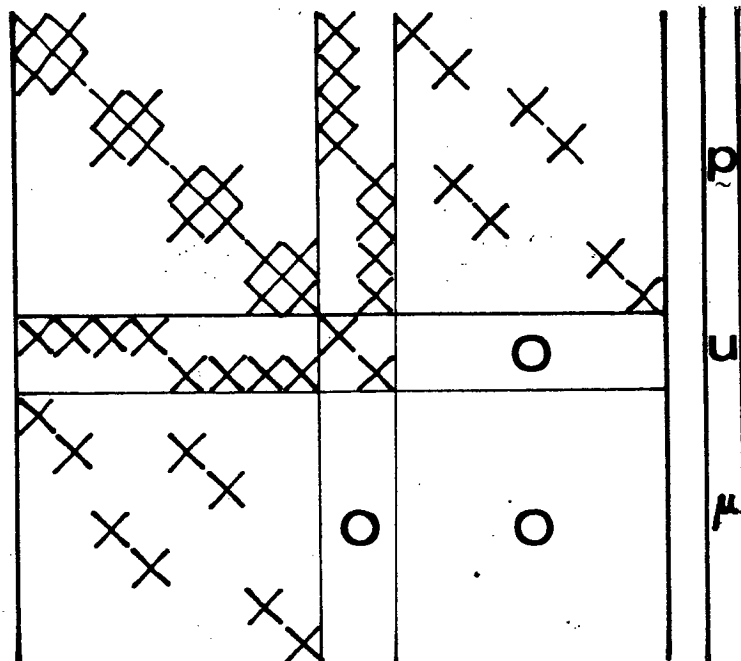
**MIXED****MIXED HYBRID**

FIGURE 1. Structure of the algebraic systems arising with the mixed and mixed-hybrid formulation

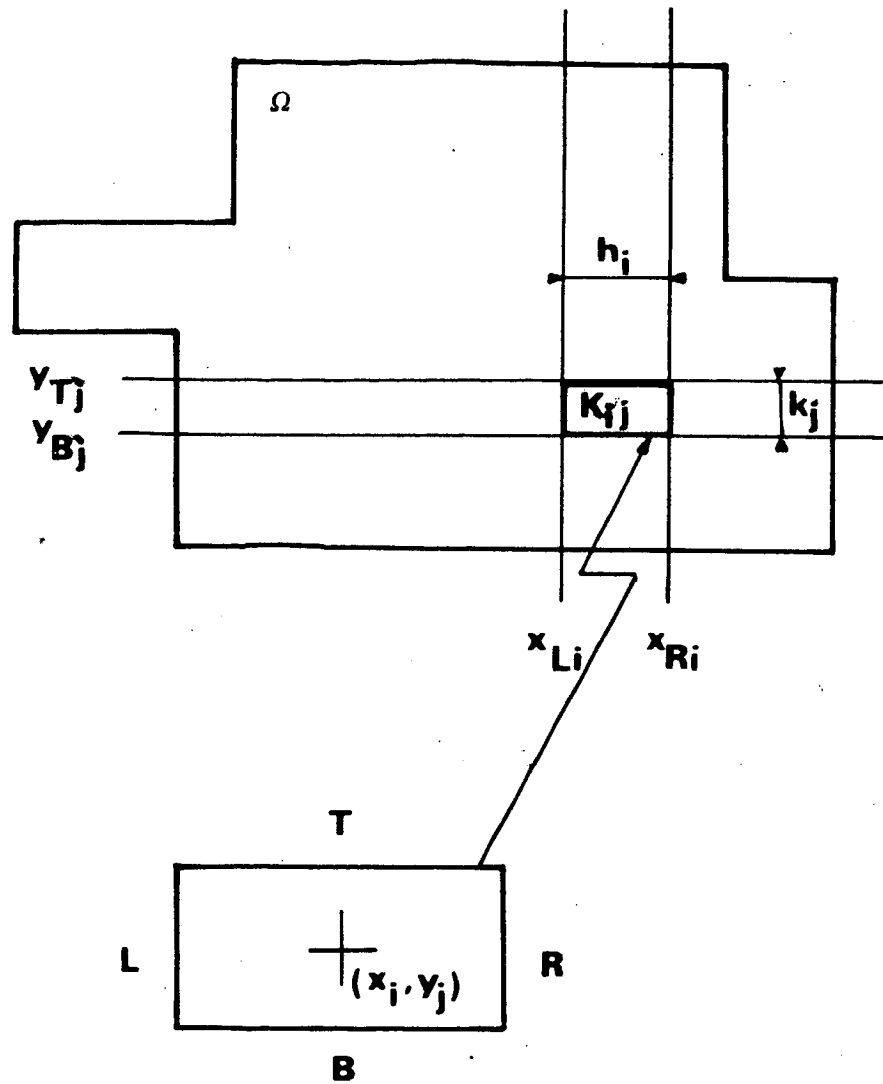


FIGURE 2. Dimensionally reduced nodal methods





